Effects of temperature and thermal cycles on the elastic shear modulus of saturated clay

Authors: O. T. Bentil and C. Zhou*

*Corresponding author

Name: Obed Takyi Bentil

Title: PhD Student

Affiliation: Department of Civil and Environmental Engineering, The Hong Kong Polytechnic University, Hung Hom, Kowloon, Hong Kong

Email: o-t.bentil@connect.polyu.hk

Name: Chao Zhou

Title: Assistant Professor

Affiliation: Department of Civil and Environmental Engineering, The Hong Kong Polytechnic University, Hung Hom, Kowloon, Hong Kong

Email: c.zhou@polyu.edu.hk

ABSTRACT

Thermo-mechanical behaviour of soils has attracted great attention in recent years, because of its great importance in some emerging geotechnical applications such as energy piles. So far, the thermo-plasticity (e.g., the influence of temperature on the yield surface) has been well understood, but the thermo-elasticity has not been purposely studied. In this study, a temperature-controlled oedometer equipped with bender elements was developed and then used to mainly investigate effects of temperature and thermal cycles on the elastic shear modulus (G_0) of a saturated lateritic clay. In addition, one test was performed on kaolin clay to investigate the influence of thermal cycles on G_0. Two types of thermo-mechanical paths were considered at different temperatures (5-60ºC) and stresses (30-400 kPa), including constant-temperature loading-unloading and constant-stress cyclic heating-cooling. Results from these tests consistently reveal that at a given stress, G_0 is smaller at a higher temperature. This can be attributed to the reduction of interparticle force during the heating of saturated clay, according to the double layer theories. Furthermore, G_0 of the lateritic clay increases by about 12% and 16% after four thermal cycles for overconsolidated and normally consolidated specimens, respectively. This can be due to soil densification and particle rearrangement during the heating-cooling cycles. These results are useful for improving the modelling of thermo-elasticity and also for the analysis of thermally active structures such as energy piles.

KEYWORDS

Temperature; thermal cycles; elastic shear modulus; lateritic soil; clays.

INTRODUCTION

Thermal effects on soil behaviour have attracted great attention in recent years because of their relevance to some emerging research areas like energy geo-structures (Laloui and Di Donna 2013; McCartney et al. 2016). Most of the previous studies focused on temperature effects on the shear strength, yielding and thermal strain of soil (Abuel-Naga et al. 2007; Cekerevac and Laloui 2004; Ghahremannejad 2003; Graham et al. 2001; Hueckel and Baldi 1990; Ng et al. 2017, 2019b; Pan et al. 2020). Some valuable findings have been reported in the literature. For example, it is well recognized that the thermal strain of soil is greatly dependent on the overconsolidation ratio (OCR). Normally consolidated and slightly overconsolidated soils generally show irreversible contraction under heating and thus lead to thermal hardening. With increasing number of thermal cycles, there is an accumulation of plastic deformation at a decreasing rate (Campanella and Mitchell 1968; Di Donna and Laloui 2015). In contrast, heavily overconsolidated soil exhibits reversible expansion during the heating process. It has been also found that the yield stress decreases with an increase in temperature at overconsolidated state, which is commonly referred to as thermal softening (Cekerevac and Laloui 2004, Tang et al. 2008).

So far, very little attention has been paid to the influence of temperature and thermal cycles on soil stiffness, which is crucial for analysing the serviceability limit state of energy piles, underground thermal energy storage facilities, etc. Cekerevac and Laloui (2004) carried out a series of triaxial tests to determine the secant Young’s modulus of a saturated kaolin clay at an axial strain of 0.5%. They considered two temperatures (i.e. 22 and 90°C) and seven over consolidation ratios (OCRs) ranging from 1 to 12. All specimens had a preconsolidation pressure of 600 kPa. It was observed that at each OCR, the secant modulus slightly increased with a temperature increase from 22 to 90°C. Zhou et al. (2015) measured the secant shear modulus of a silt from Hong Kong in the strain range of 0.003% to 1% at 20 and 60°C. All specimens were normally consolidated with a preconsolidation pressure of 100 kPa. When the deviator strain was less than 0.3%, the modulus at 60°C was consistently lower than that at 20°C and the difference was smaller at a higher strain. When the deviator strain was higher than 0.3%, the thermally induced difference was negligible. Note that the above contradictory results cannot be well explained by the influence of OCR, because Cekerevac and Laloui (2004) reported consistent results at various OCRs. The contradiction may be attributed to the differences of stresses, temperatures and strains in the two studies. A possible reason is that Cekerevac and Laloui (2004) applied a larger temperature increment and used a soil with a higher plasticity. The heating-induced volumetric contraction was about five times of that in the study of Zhou et al. (2015). Therefore, in the study of Cekerevac and Laloui (2004), heating-induced soil densification played a more important role, compensated other effects of temperature such as thermal softening, and resulted in a higher modulus at 90°C. In addition, the data of Zhou et al. (2015) revealed that thermal effects on soil stiffness are strain-dependent. The conclusion about secant modulus may depend on the strain level. It should be pointed out further studies are required to verify the above postulations and fully understand the coupled influence of OCR, stress, temperature and strain on soil stiffness.

The above studies of soil stiffness focused on the secant modulus, which is likely affected by both thermo-elasticity and thermo-plasticity (e.g. thermal effects on yielding and dilatancy), rather than the elastic stiffness at very small strains (typically below 0.001%). A good understanding of the elastic shear modulus G_0 is important for several reasons. Firstly, G_0 is an important parameter for predicting the ground movement and the serviceability limit state of geo-structures. Secondly, G_0 is a critical parameter to model the degradation curve of shear modulus with strain (Ng et al. 2015) which is often used in the geotechnical analysis. Lastly, the elastic law is an important component in elastoplastic constitutive models. Only recently, Vahedifard et al. (2020) measured G_0 of a silt using bender elements in a temperature-controlled triaxial. They found that G_0 decreased as soil temperature increased from 23 to 43°C. Their study mainly focused on unsaturated conditions and the explanations of experimental results were mainly based on thermal effects on the air-water surface tension. There are only two data points at saturated condition and therefore no solid conclusion can be drawn for saturated soils. Moreover, to the best of the authors' knowledge, there is no study of the cyclic thermal effects on G_0 in the literature.

In this study, a new temperature-controlled oedometer equipped with bender elements was developed. Using this apparatus, a saturated and compacted lateritic clay was mainly tested to investigate temperature and thermal cycles effects on the G_0. In addition, one test was carried out to study the influence of thermal cycles on G_0 of kaolin clay.

TESTING APPARATUS

A new temperature-controlled oedometer equipped with bender elements was developed in this study, as shown in Figure 1. To control soil temperature, it used a temperature control system manufactured by PolyScience to circulate heated/cooled water in a spiral copper tube surrounding the specimen. A thermocouple was installed inside the oedometer to monitor soil temperature. To minimize the energy loss, an insulating material was used to wrap the oedometer. Based on a calibration test equipped with three thermocouples (one in the specimen centre, one at the specimen edge and the last one in the water surrounding the oedometer), 6 hours were sufficient to achieve a steady and uniform temperature in the specimen. The accuracy of temperature control was 0.1°C. In addition, bender elements were applied to measure the shear wave velocity and then calculate G_0.

It should be noted that the temperature change may have an impact on the measuring devices such as bender element and dial gauge. Some calibration/trial tests were carried out to address this problem. On the one hand, a calibration test was carried out to determine the influence of thermal expansion/contraction of the oedometer and loading rod on the dial gauge.

The apparatus without a specimen was subjected to several heating-cooling cycles, during which the reading of dial gauge was monitored and used to correct the measured thermal strain of soil specimen. In addition, a long loading rod was purposely used to minimize the temperature variation of dial gauge pin. On the other hand, it was found from some trial tests that the bender element works well when the temperature is below 60°C. At temperatures above 60°C, the quality of received signal begins to reduce with increasing temperature. This can be attributed to an increase in the electrical resistance of the wires connected to the bender element. Hence, temperatures considered in the test program do not exceed 60°C. Moreover, after thermal and mechanical equilibrium at each test condition, several wave propagation measurements were done. The variability of shear wave velocities is less than 1%.

TEST SOIL, PROGRAM AND PROCEDURES

A lateritic clay was tested in this study. Its basic properties are summarized in Table 1 and detailed description of this soil was reported by Ng et al. (2019). Soil specimens were statically compacted at 19.5% water content (i.e., the optimum moisture content (OMC)). The density was 1.62 g/cm^3 dry density (void ratio of 0.65), corresponding to 95% of the maximum dry density (MDD) obtained from the standard proctor compaction. The diameter and height of each specimen were 150 and 60 mm, respectively. To saturate the specimens, they were submerged in water for 48 hours at a low vertical effective stress of about 12 kPa.

Two types of stress- and temperature-controlled tests were carried out using the lateritic clay. First of all, two 1D compression tests were performed at 5 and 40ºC, as shown in Figure 2(a). In each test, the predefined temperature was firstly applied (i.e., O-A and O-B). After thermal equalisation, the vertical effective stress was increased from 30 to 400 kPa stepwise and then decreased to 30 kPa (as indicated by the short dashes and solid symbol between A-A2 and B-B2, respectively). The consolidation in each stage was considered to be completed when the dial gauge reading stayed constant for 24 hours. Secondly, two cyclic heating-cooling tests in the temperature range of 5 to 60ºC were carried out at 50 and 400 kPa (Figure 2(b)). The ranges of stress and temperature were selected with reference to energy piles (Brandl 2006; Laloui and Sutman 2021; Lv et al. 2020), although the results may be applicable to other energy geo-structures. The specimens were loaded to the desired stress (i.e., O-C and O-D, respectively) at room temperature and then subjected to three heating-cooling cycles stepwise (i.e., C-C1-C2 and D-D1-D2 for each cycle, respectively). Six temperature stages were considered, including 5, 20, 30, 40, 50 and 60ºC. Each temperature stage was maintained for 12 hours to ensure that the specimen reached an equilibrium state. In addition, the vertical deformation of soil specimen was monitored in all tests by a dial gauge. At the desired thermo-mechanical states indicated by markers in Figure 2, bender element tests were performed to measure the shear wave velocity to estimate G_0.

In addition to the tests on the lateritic clay, a test was carried out on Speswhite kaolin to investigate the influence of thermal cycles on G_0. The clay compacted at the OMC (i.e., 29.5%) and to 95% MDD and then saturated. After that, the specimen was subjected to three heating-cooling cycles in the temperature range of 5 to 60ºC at a vertical effective stress of 400 kPa. Only two temperature stages (5 and 60ºC) were considered in the process of cyclic heating-cooling to reduce the test duration.

EXPERIMENTAL RESULTS

Figure 3(a) shows the two compression curves at temperatures of 5 and 40ºC. They are almost the same in the stress range below 200 kPa. On the contrary, the specimen at 40ºC becomes more compressible than that at 5ºC above 200 kPa. During unloading, the two specimens show a similar swelling index. Figure 3(b) shows G_0 measured in these two tests. It can be seen that the G_0 at 40ºC are consistently lower than those at 5ºC during both loading and unloading, even though the specific volume is lower at 40ºC because of the thermal effects on soil compressibility. The maximum difference in G_0 is about 10% during loading (see the data points at 100 kPa). During unloading, the maximum difference is up to 30% (at 30 kPa). As discussed above, previous studies of thermal effects on soil stiffness in the literature (Vahedifard et al. 2020; Zhou et al. 2015) only considered a single stress condition. The new results of this study suggest that the significance of thermal effects was highly stress path dependent.

Figure 4 shows the volumetric strain of the specimens subjected to cyclic heating and cooling at vertical effective stresses of 50 and 400 kPa. With regards to results at 400 kPa, the first cooling from 20 to 5ºC induces a small contractive strain of 0.01%. Upon heating from 5 to 20ºC, an additional contractive strain of 0.09% occurs. When the temperature further increases to 60ºC, the contractive strain increases to 0.44%. During the subsequent heating-cooling cycles, the specimen continues to contract. After four thermal cycles, the accumulated strain is up to 0.66%. The results at 50 kPa are similar to those at 400 kPa, but the thermal strains are much smaller. The difference is mainly because the specimens at 400 and 50 kPa are normally consolidated and overconsolidated, respectively. Similar findings were reported in the literature (Abuel-Naga et al. 2007; Di Donna and Laloui 2015).

Figure 5(a) shows G_0 measured during the thermal cycles at 400 kPa. G_0 decreases during heating and increases during cooling. This is consistent with the finding from Figure 3, implying that the observed temperature effects are applicable to different thermo-mechanical paths. Figure 5(b) shows the variation of G_0 during heating-cooling cycles at 50 kPa, with a trend similar to that at 400 kPa.

Figure 6 shows G_0 and thermal strain measured at 5ºC but after thermal cycles. At both 400 and 50 kPa, G_0 of the lateritic clay consistently increased after thermal cycles. This is very likely due to heating/cooling cycles-induced soil densification and particle rearrangement. When the vertical effective stresses are 400 and 50 kPa, G_0 increased by about 16% and 12% after four thermal cycles, respectively. The difference is most probably because the contractive thermal strain is much larger at 400 kPa. Results of the kaolin clay are also included in Figure 6. It can be seen that the thermal cycles result in an increase in G_0 by about 30%, similar to that of the lateritic clay.

DISCUSSION

Effects of temperature, thermal cycles, stress and thermo-mechanical path on G_0

Based on the results shown in the previous section, several important findings can be obtained. Firstly, G_0 would decrease with an increase in temperature (Figures 3(b) and 5), at least for the tested lateritic clay. This can be attributed to the influence of temperature on the interparticle force of saturated clay (Laloui 2001). As suggested by the double layer theories (Israelachvili 2011), an increase in soil temperature would reduce the electrical repulses force between soil particles, thereby causing a reduction of G_0. Secondly, G_0 increases with an increasing number of thermal cycles (Figure 6), particularly for normally consolidated soil. This is at least partially due to the irreversible contractive strain accumulated during the heating-cooling cycles. Thirdly, as expected, G_0 increases with an increase in effective stress (Figures 3(b). This is well expected, because an increase in effective stress can enhance the inter-particle contact.

The preliminary data implies that a switch of the mechanical and thermal loading paths is likely to affect G_0. For example, the specimens at point A1 in Figure 2(a) and point C1 in Figure 2(b) have the same effective stress and temperature, but their G_0 are different by 8%. The specimen subjected to a compression-cooling path shows a larger G_0 than that with a cooling-compression path. This is at least partially because the former specimen was compressed at a higher temperature, resulting in a larger reduction of void ratio. In addition, further work is recommended to investigate the path dependency with consideration of more mechanical and thermal paths.

Discussion on the existing formulations for temperature-dependent G_0

The findings from this study can be readily applied in the theoretical modelling of soil behaviour. So far, many thermo-mechanical models have been reported in the literature within the elastoplastic framework. The thermo-plasticity have been well understood and incorporated in the models (Abuel-Naga et al. 2009; Graham et al. 2001; Hamidi et al. 2014; Hueckel and Baldi 1990; Zhou and Ng 2015). However, the existing models do not consider thermal effects on the elastic behaviour due to the lack of experimental data, except the models reported by Graham et al. (2001) and Hamidi et al. (2014). Even though these two models have incorporated thermal effects on the G_0, the relevant formulations were not verified using experimental results. The results from this study may give some insights to their formulations for G_0. Since their G_0 formulations are similar, only the one by Hamidi et al. (2014) is discussed here:

$$G_{T(OC)} = G_{T_0(NC)} \left(\frac{p'}{p'_c}\right)^b \left[1 + D ln\left(\frac{T}{T_0}\right)\right] \quad (1)$$

where $G_{T(OC)}$ is the shear modulus of overconsolidated soil at a temperature T; $G_{T_0(NC)}$ is the shear modulus of normally consolidated soil at a reference temperature T_0; p'_c is the preconsolidation stress; p' is the current effective mean stresses; and D and b are model parameters. Based on the experimental results shown in Figure 5, G_0 can be either larger or small when the temperature is higher, depending on soil type, temperature range, etc. In addition, the equation suggests that the effects of temperature and OCR are independent, whereas the observed thermal effects are more significant when the OCR is lower (see Figure 5). The above analysis illustrates that D is a function of several factors such as soil type, temperature range and OCR rather than a constant value. More experimental results are required to fully understand the evolution of D.

Potential applications of temperature-dependent G_0 in the geotechnical analysis

There are very limited studies of G_0 at non-isothermal conditions in the literature, but it is an important parameter in many methods of analyzing thermally active structures like energy piles. For the soils surrounding energy piles, they are subjected to heating-cooling cycles. Ng et al. 2015) derived an analytical solution to predict the influence of temperature on the shaft resistance of energy piles based on the cavity expansion theory. In their solution, the shear modulus of soil is dependent on two factors, including G_0 and the stiffness degradation rate with strain. The value of G_0 (typically in the range below 0.001%) would affect the predicted shear modulus at various strains, so G_0 is a crucial input parameter. This study provides useful experimental data to reveal the influence of temperature and thermal cycles on G_0. When the operational temperature of energy piles increases from 5 to 40ºC in a typical range, the reduction of G_0 can be up to 30% (Figure 3(b)). It would be more conversative to adopt the value of G_0 measured at the highest operational temperature in the design of energy piles. Moreover, G_0 increases as the number of thermal cycles increases (Figure 6). This would be beneficial to the long-term performance of energy piles. In addition, the progressive thermal contraction of soils (Figure 4) could reduce the normal force at pile-soil interfaces and therefore induce additional pile settlement.

Note that the above observations and discussion should be treated with caution, since they may be specific and only applicable to some soil types. Experimental data in the literature suggest that the thermo-mechanical behaviour of fine-grained soils are qualitatively similar. At a quantitative level, some researchers (Abuel-Naga et al. 2007; Di Donna and Laloui 2015; Ng et al. 2020; Sultan et al. 2002) correlated the plastic index (PI) and thermal effects on soil behaviour. When the PI of a soil is higher, its behaviour is more sensitive to the change in temperature. Further studies are recommended to examine G_0 for a variety of soils.

CONCLUSIONS

When the temperature increases from 20 to 40ºC, the decrease in the elastic shear modulus G_0 is up to 30% for the tested lateritic clay. This may be because the heating causes an increase in the electric repulsive force between soil particles. Consequently, the shear wave velocity and hence the G_0 become smaller.

After four thermal cycles in the temperature range of 5 and 60ºC, the G_0 increases by 12% and 16% for lateritic specimens loaded at 50 and 400 kPa, respectively. Under the same thermal cycles, G_0 increases by about 30% for the kaolin clay loaded at 400 kPa. The increase is mainly attributed to soil densification and particle rearrangement induced by heating-cooling cycles.

These above results provide experimental evidence to improve the modelling of thermo-elasticity in constitutive models and the analysis of thermally active geo-structures.

DATA AVAILABILITY STATEMENT

All data, models, and code generated or used during the study appear in the submitted article.

ACKNOWLEDGEMENTS

This work is supported by the National Science Foundation of China through the research grant 52022004. The authors also would like to thank the Research Grants Council (RGC) of the HKSAR for providing financial support through the grants 16216116 and AoE/E-603/18.

REFERENCES

Abuel-Naga, H. M., Bergado, D. T., Bouazza, A., and Pender, M. (2009). "Thermomechanical model for saturated clays." *Geotechnique*, 59(3), 273–278.

Abuel-Naga, H. M., Bergado, D. T., Bouazza, A., and Ramana, G. V. (2007). "Volume change behaviour of saturated clays under drained heating conditions: experimental results and constitutive modeling." *Canadian Geotechnical Journal*, 44(8), 942–956.

Brandl, H. (2006). "Energy foundations and other thermo-active ground structures." *Geotechnique*, 56(2), 81–122.

Campanella, R. G., and Mitchell, J. K. (1968). "Influence of Temperature Variations on Soil

Behavior." *Journal of the Soil Mechanics and Foundations Division*, American Society of Civil Engineers (ASCE), 94(3), 709–734.

Cekerevac, C., and Laloui, L. (2004). "Experimental study of thermal effects on the mechanical behaviour of a clay." *International Journal For Numerical And Analytical Methods In Geomechanics*, John Wiley and Sons Ltd, 28(3), 209–228.

Di Donna, A., and Laloui, L. (2015). "Response of soil subjected to thermal cyclic loading: Experimental and constitutive study." *Engineering Geology*, Elsevier, 190, 65–76.

Ghahremannejad, B. (2003). "Thermo-mechanical behaviour of two reconstituted clays." PhD thesis. University of Sydney.

Graham, J., Tanaka, N., Crilly, T., and Alfaro, M. (2001). "Modified Cam-Clay modelling of temperature effects in clays." *Canadian Geotechnical Journal*, 38(3), 608–621.

Hamidi, A., Asce, A. M., Tourchi, S., Asce, S. M., and Khazaei, C. (2014). "Thermomechanical Constitutive Model for Saturated Clays Based on Critical State Theory."

Hueckel, T., and Baldi, G. (1990). "Thermoplasticity of Saturated Clays: Experimental Constitutive Study." *Journal of Geotechnical Engineering*, 116(12), 1778–1796.

Israelachvili, J. (2011). *Intermolecular and surface forces*. 3rd Edition. Academic Press, New York.

Laloui, L. (2001). "Thermo-mechanical behaviour of soils." *Environmental geomechanics.*, EPFL Press, Lausanne, 5(6), 809–843.

Laloui, L., and Di Donna, A. (2013). *Energy Geostructures*. *Energy Geostructures: Innovation in Underground Engineering*, (L. Laloui and A. Di Donna, eds.), John Wiley & Sons, Inc., Hoboken, NJ USA.

Laloui, L., and Sutman, M. (2021). "Experimental investigation of energy piles: From laboratory to field testing." *Geomechanics for Energy and the Environment*, Elsevier, 27, 100214.

Lv, Z., Kong, G., Liu, H., and Ng, C. W. W. (2020). "Effects of Soil Type on Axial and Radial Thermal Responses of Field-Scale Energy Piles." *Journal of Geotechnical and Geoenvironmental Engineering*, American Society of Civil Engineers, 146(10), 06020018.

McCartney, J. S., Sánchez, M., and Tomac, I. (2016). "Energy geotechnics: Advances in subsurface energy recovery, storage, exchange, and waste management." *Computers and Geotechnics*, Elsevier Ltd, 75, 244–256.

Ng, C. W. W., Akinniyi, D. B., and Zhou, C. (2020). "Volume change behaviour of a saturated lateritic clay under thermal cycles." *Bulletin of Engineering Geology and the*

Environment, 80(1), 653–661.

Ng, C. W. W., Akinniyi, D. B., Zhou, C., and Chiu, C. F. (2019a). “Comparisons of weathered lateritic, granitic and volcanic soils: Compressibility and shear strength.” *Engineering Geology*, Elsevier B.V., 249, 235–240.

Ng, C. W. W., Mu, Q. Y., and Zhou, C. (2017). “Effects of boundary conditions on cyclic thermal strains of clay and sand.” *Géotechnique Letters*, 7(1), 73–78.

Ng, C. W. W., Mu, Q. Y., and Zhou, C. (2019b). “Effects of specimen preparation method on the volume change of clay under cyclic thermal loads.” *Géotechnique*, 69(2), 146–150.

Ng, C. W. W., Shi, C., Gunawan, A., Laloui, L., and Liu, H. L. (2015). “Centrifuge modelling of heating effects on energy pile performance in saturated sand.” *Canadian Geotechnical Journal*, 52(8), 1045–1057.

Pan, Y., Coulibaly, J. B., and Rotta Loria, A. F. (2020). “Thermally induced deformation of coarse-grained soils under nearly zero vertical stress.” *Géotechnique Letters*, 10(4), 486–491.

Sultan, N., Delage, P., and Cui, Y. J. (2002). “Temperature effects on the volume change behaviour of Boom clay.” *Engineering Geology*, Elsevier, 64(2–3), 135–145.

Tang, A.-M., Cui, Y.-J., and Barnel, N. (2008). “Thermo-mechanical behaviour of a compacted swelling clay.” 58(1), 45–54.

Vahedifard, F., Thota, S. K., Cao, T. D., Samarakoon, R. A., and McCartney, J. S. (2020). “Temperature-Dependent Model for Small-Strain Shear Modulus of Unsaturated Soils.” *Journal of Geotechnical and Geoenvironmental Engineering*, American Society of Civil Engineers (ASCE), 146(12), 04020136.

Zhou, C., and Ng, C. W. W. (2015). “A thermomechanical model for saturated soil at small and large strains.” *Canadian Geotechnical Journal*, 52(8), 1101–1110.

Zhou, C., Xu, J., and Ng, C. W. W. (2015). “Effects of temperature and suction on secant shear modulus of unsaturated soil.” *Géotechnique Letters*, 5(3), 123–128.

Table 1 Physical properties of the lateritic soils

Index property	Value
Atterberg limits	
• Liquid limit	47
• Plasticity index	21
Particle size distribution (%)	
• Sand fraction	42
• Silt fraction	16
• Clay fraction	42
Standard Proctor compaction	
• Optimum moisture content (%)	19.5
• Maximum dry density (Mg/m^3)	1.70
Classification	
• USCS (ASTM 2017)	Sandy lean clay (CL)
Main chemical composition (%)	
• SiO_2	60
• Fe_2O_3	10
• Al_2O_3	28

Figure 1

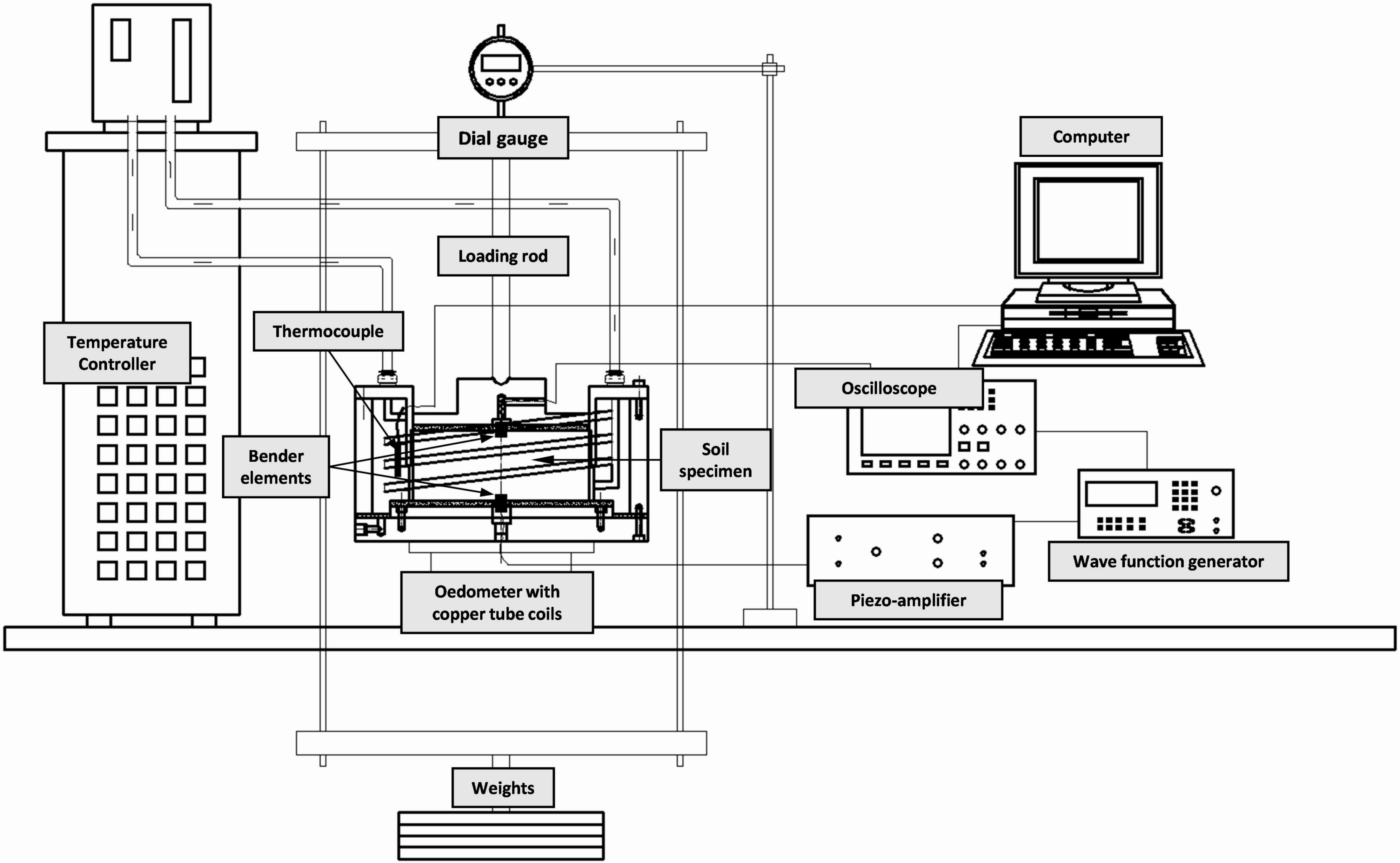

Dial gauge
Computer
Loading rod
Thermocouple
Temperature Controller
Oscilloscope
Bender elements
Soil specimen
Wave function generator
Piezo-amplifier
Oedometer with copper tube coils
Weights

Figure 2a

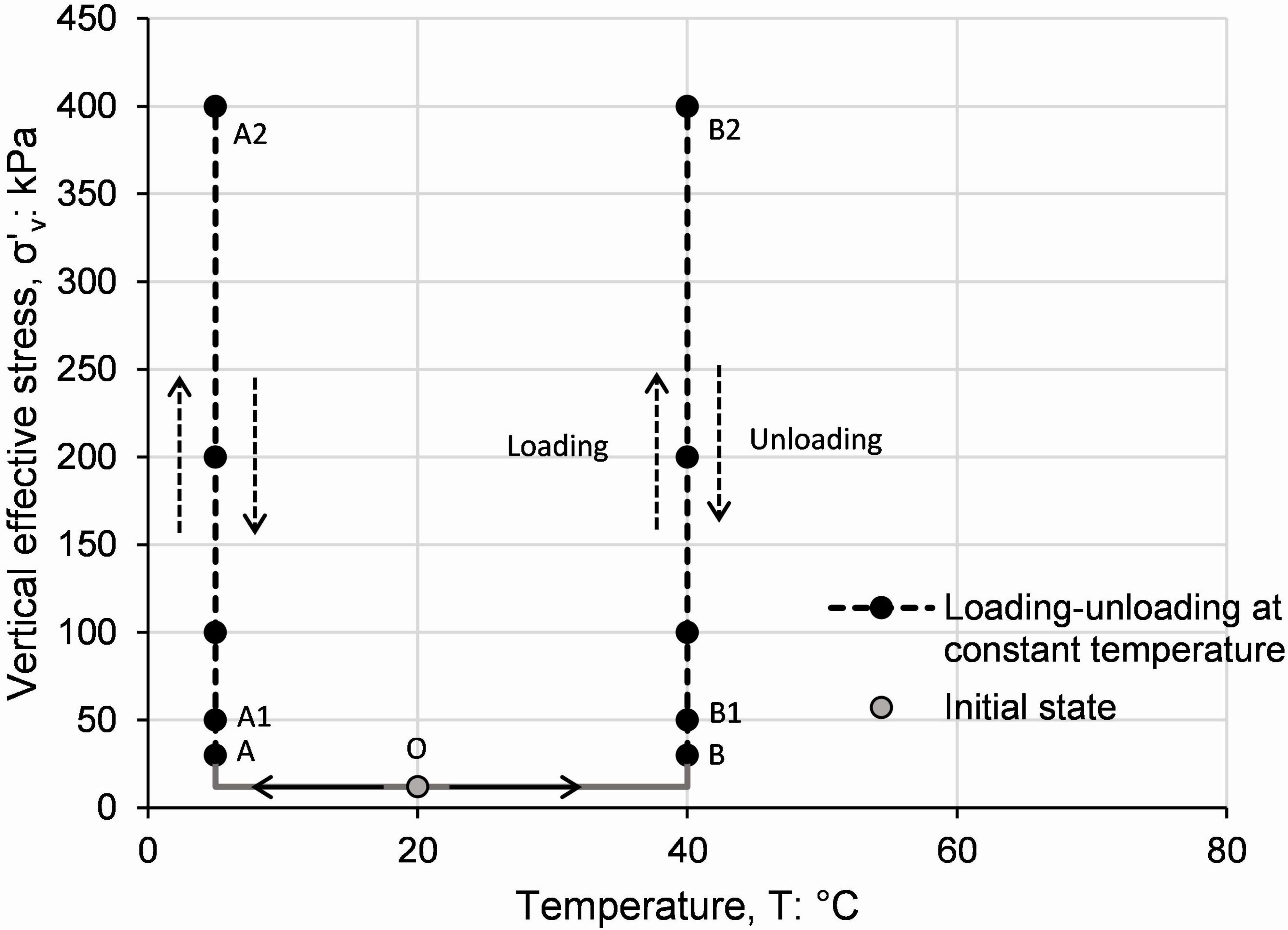
450
400
350
300
250
200
150
100
50
0
Vertical effective stress, σ'v: kPa
A2
B2
Loading
Unloading
A1
B1
A
B
O
Loading-unloading at constant temperature
Initial state
0
20
40
60
80
Temperature, T: °C

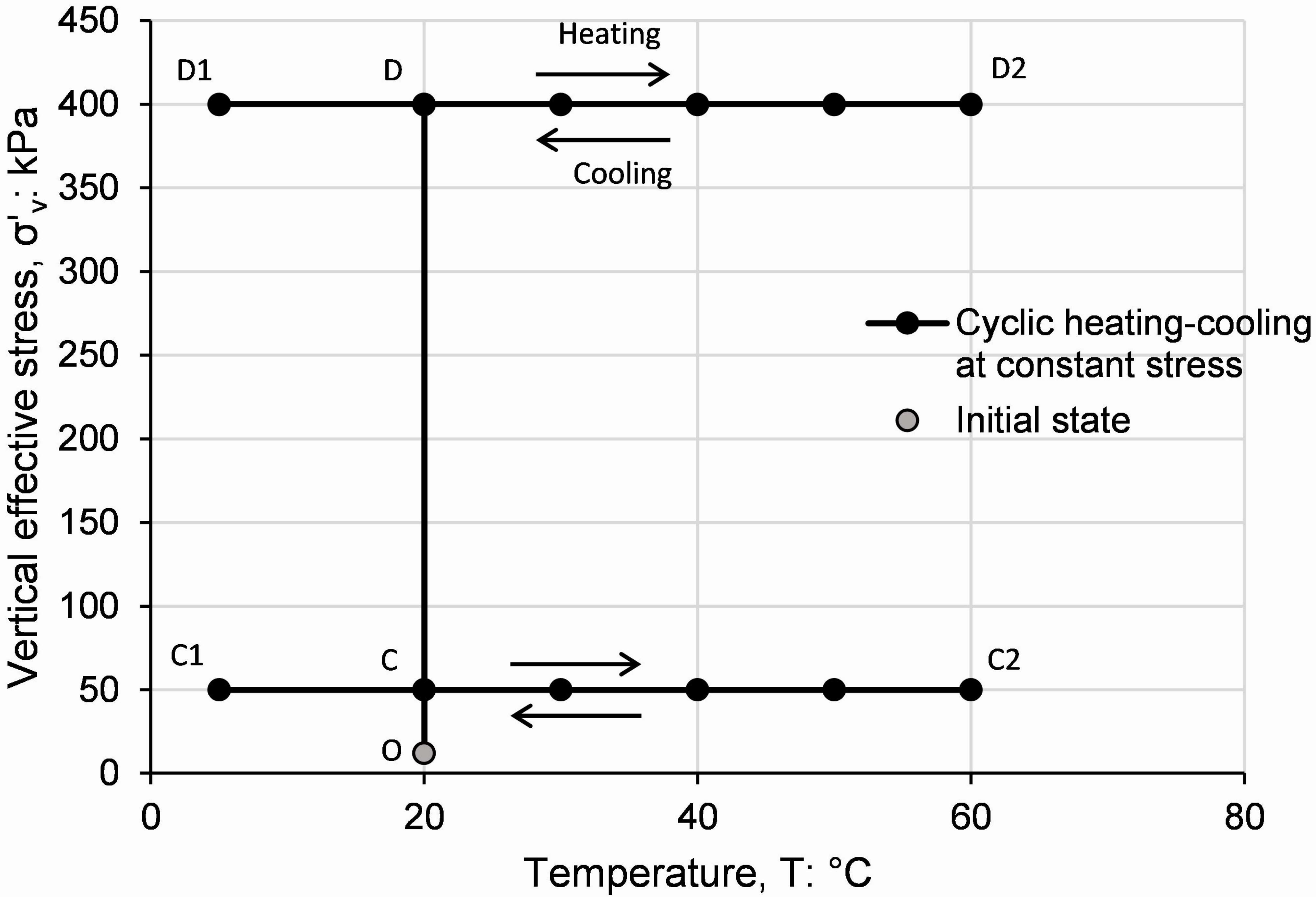

450
400
350
300
250
200
150
100
50
0
0
20
40
60
80
Vertical effective stress, σ'v: kPa
Temperature, T: °C
Heating
Cooling
D1
D
D2
C1
C
C2
O
Cyclic heating-cooling at constant stress
Initial state

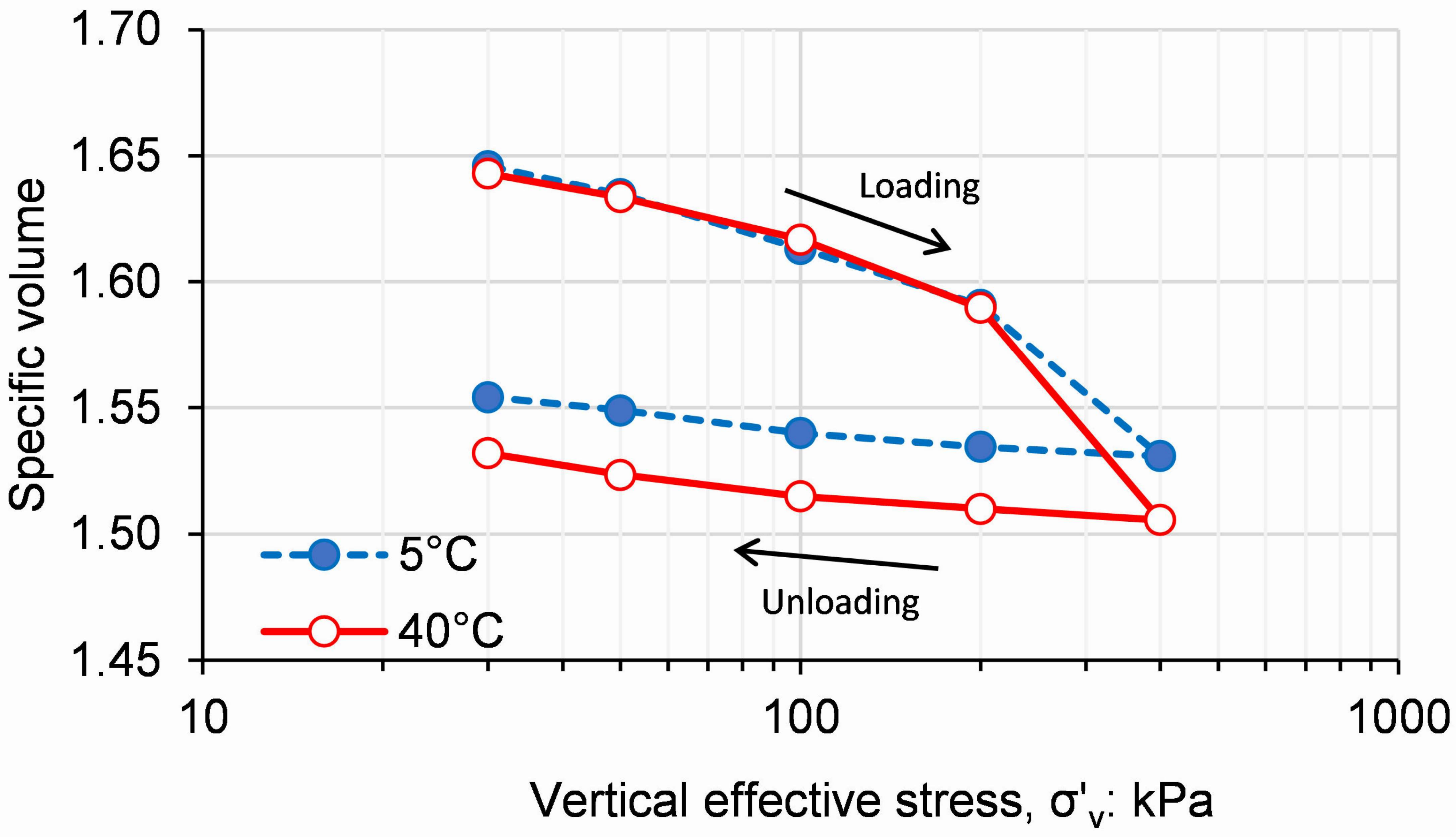
1.70
1.65
1.60
1.55
1.50
1.45
Specific volume
Loading
Unloading
5°C
40°C
10
100
1000
Vertical effective stress, σ'v: kPa

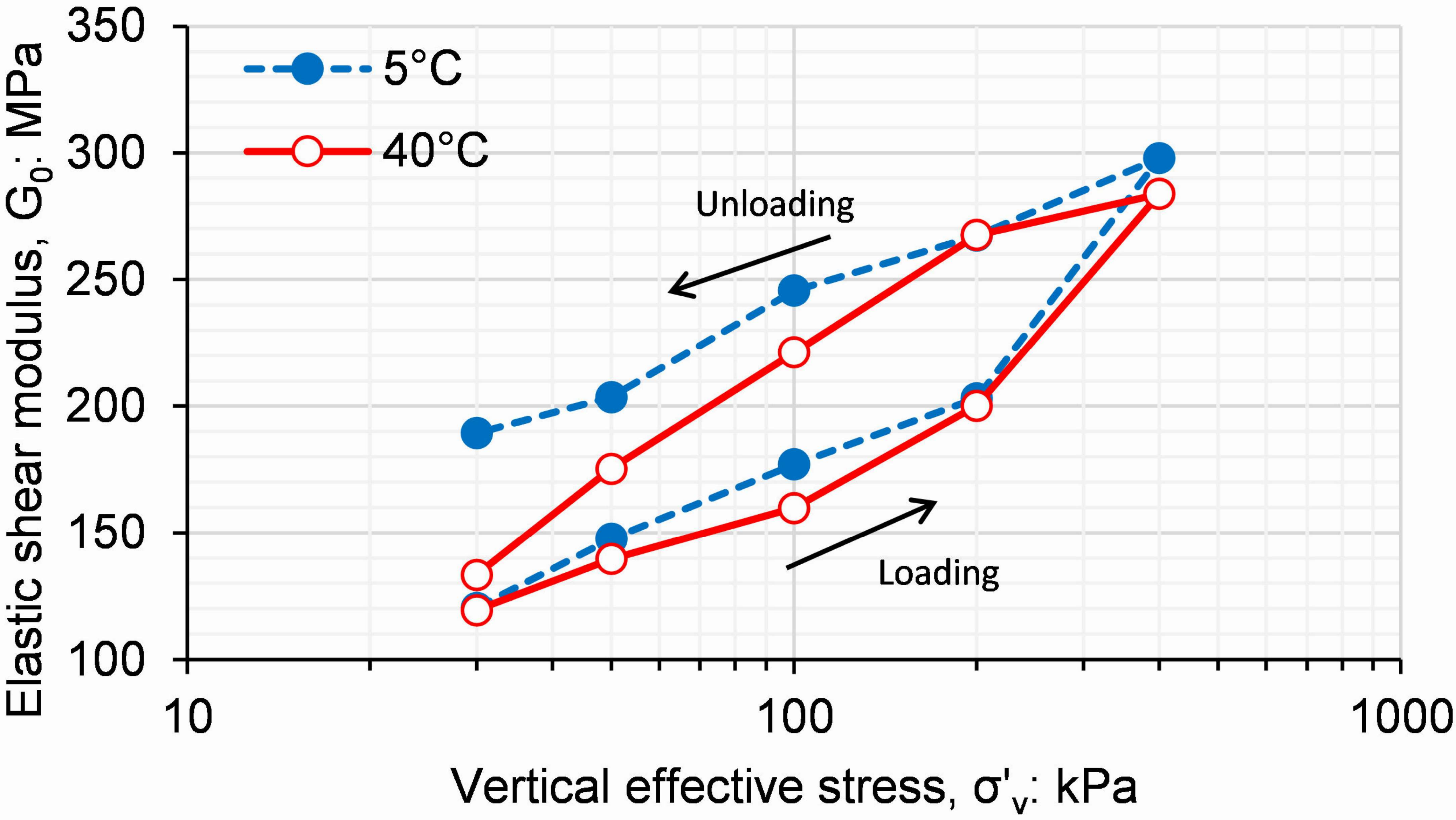
5°C
40°C
Unloading
Loading
Elastic shear modulus, G0: MPa
350
300
250
200
150
100
10
100
1000
Vertical effective stress, σ'v: kPa

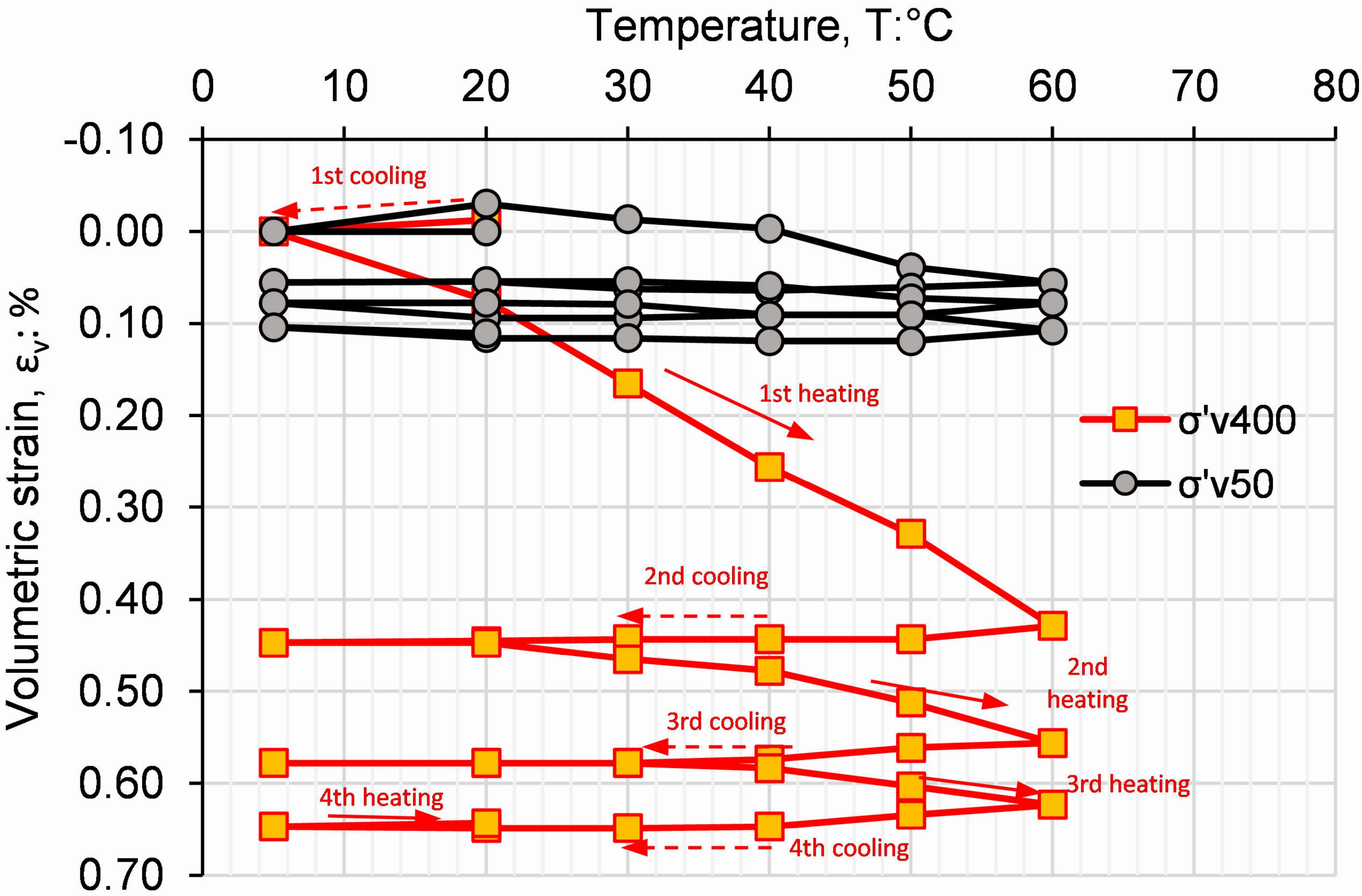

Temperature, T:°C
0
10
20
30
40
50
60
70
80
-0.10
0.00
0.10
0.20
0.30
0.40
0.50
0.60
0.70
Volumetric strain, ε_v: %
1st cooling
1st heating
2nd cooling
2nd heating
3rd cooling
3rd heating
4th heating
4th cooling
σ'v400
σ'v50

Figure 5a

Click here to access/download;Figure;Figure 5a.pdf

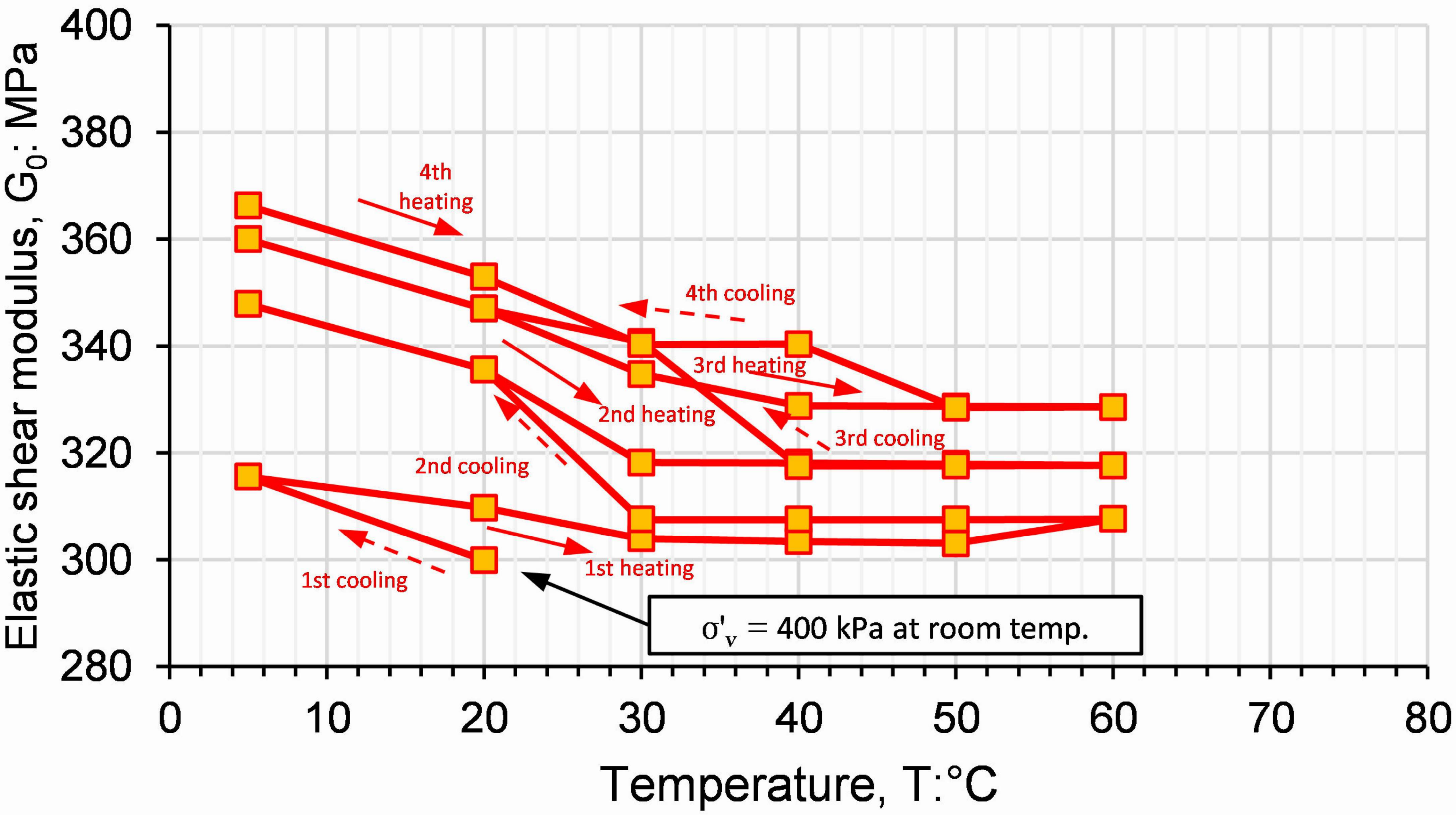

Figure 5b

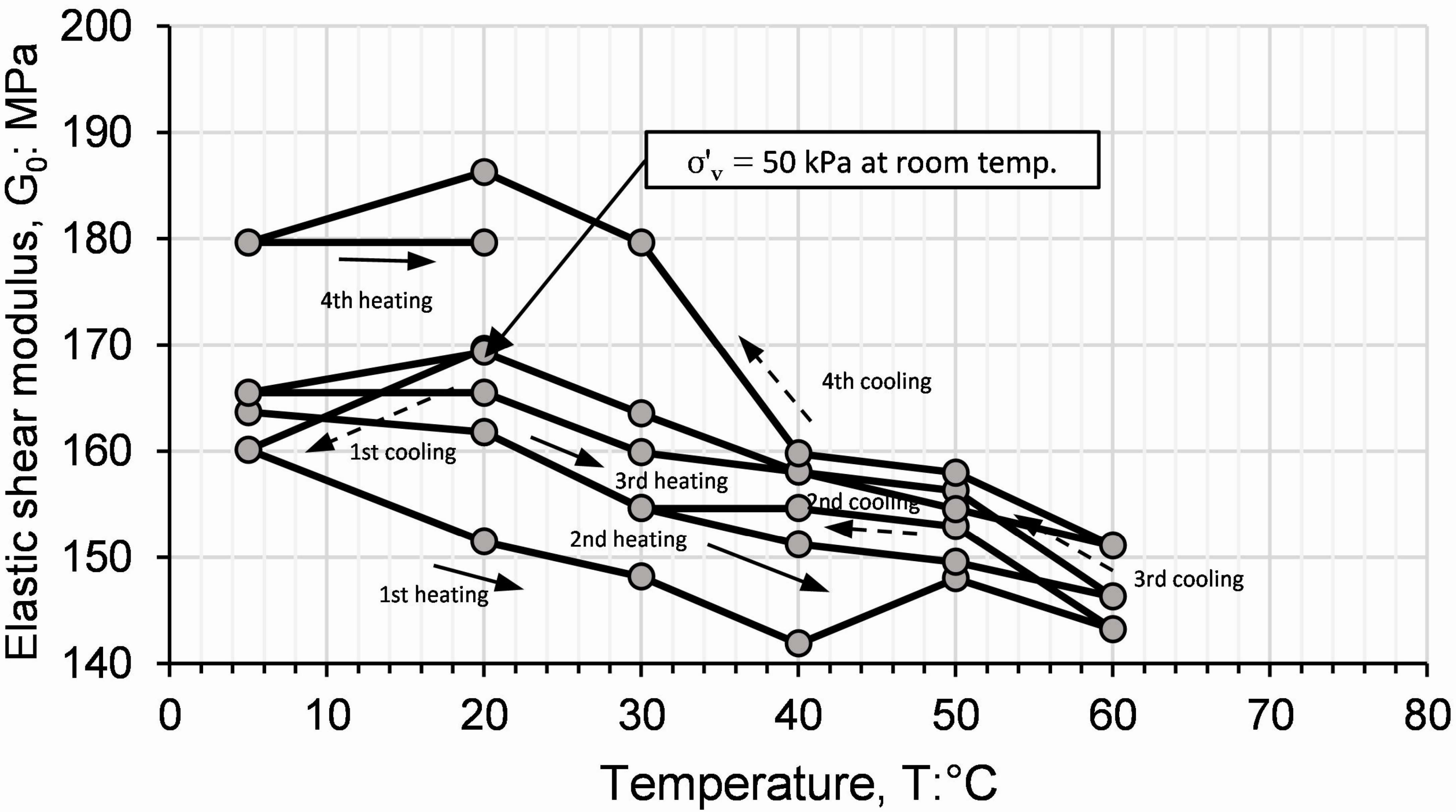
σ'v = 50 kPa at room temp.
4th heating
4th cooling
1st cooling
3rd heating
2nd cooling
2nd heating
1st heating
3rd cooling
Elastic shear modulus, G0: MPa
200
190
180
170
160
150
140
0
10
20
30
40
50
60
70
80
Temperature, T:°C

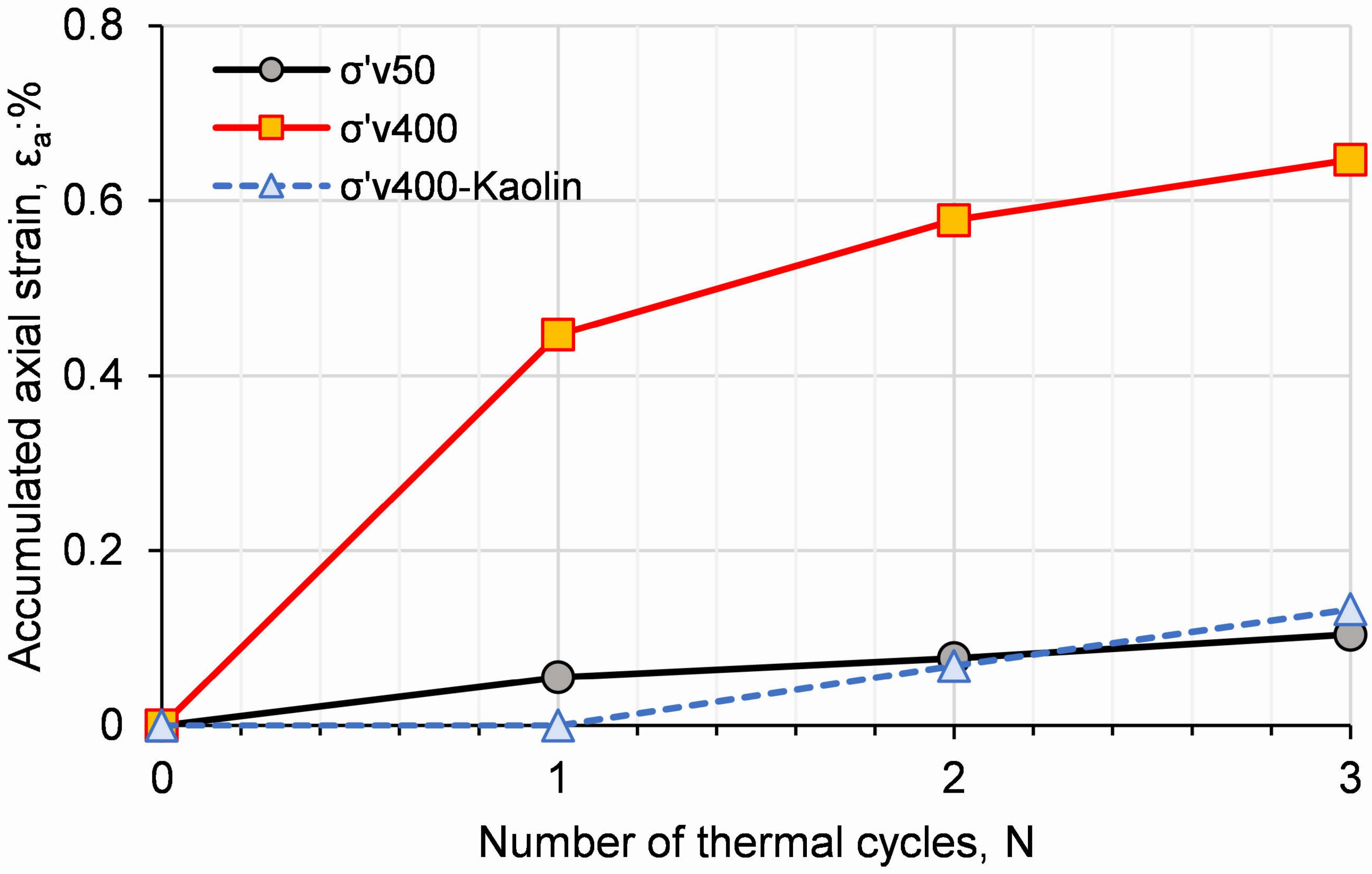
0.8
0.6
0.4
0.2
0
Accumulated axial strain, ε_a:%
σ'v50
σ'v400
σ'v400-Kaolin
0
1
2
3
Number of thermal cycles, N

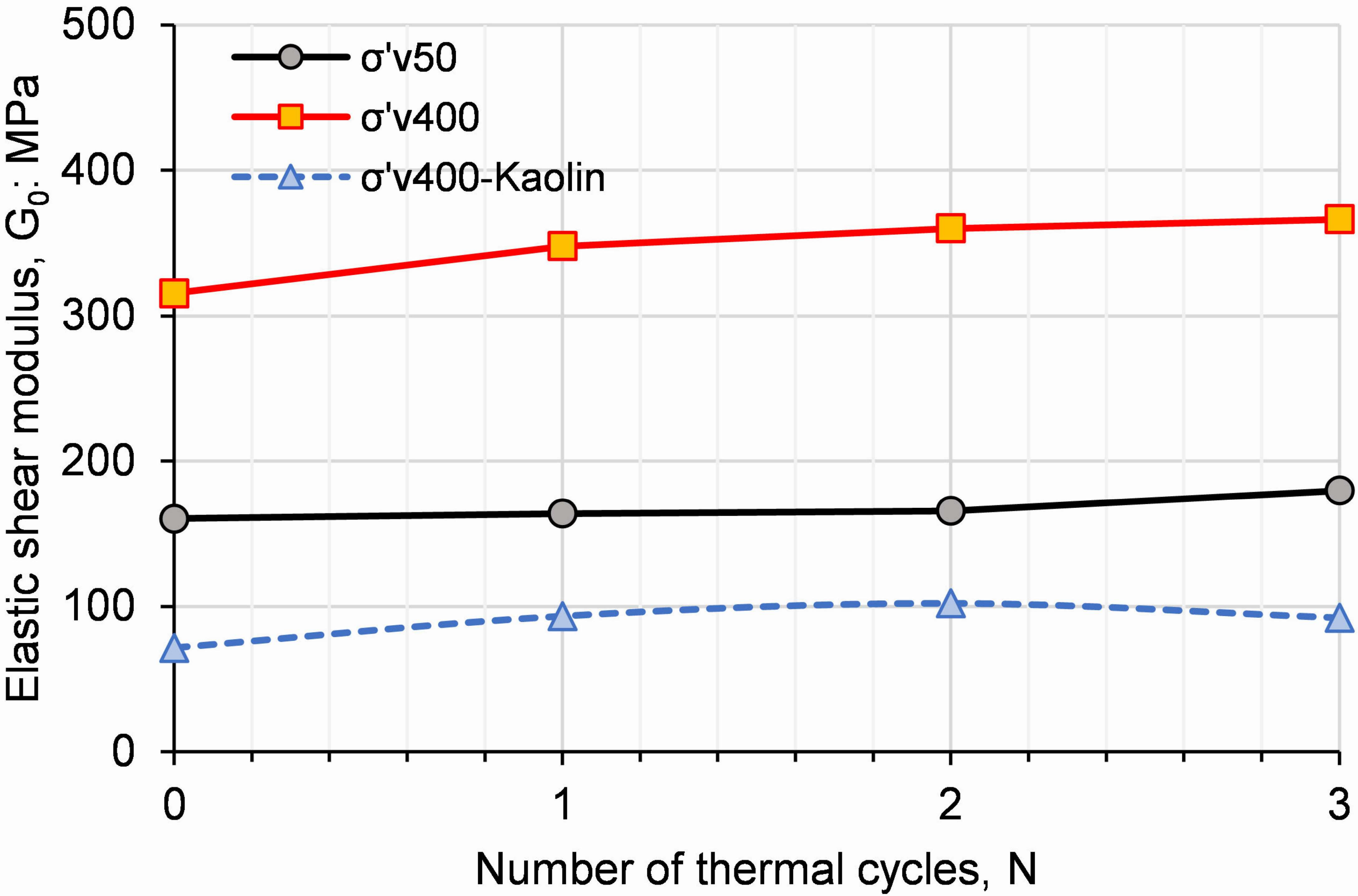

500
400
300
200
100
0
0
1
2
3
σ'v50
σ'v400
σ'v400-Kaolin
Elastic shear modulus, G_0: MPa
Number of thermal cycles, N

List of figures